J. Fluid Mech. (2003), *vol.* 494, *pp.* 141–162.
DOI: 10.1017/S0022112003005949 Printed in the United Kingdom

Excitation of trapped water waves by the forced motion of structures

By P. McIVER[1], M. McIVER[1] AND J. ZHANG[2]

[1]Department of Mathematical Sciences, Loughborough University, Loughborough, Leics, LE11 3TU, UK

[2]Department of Earth Science and Engineering, Royal School of Mines, Imperial College, Prince Consort Road, London, SW7 2BP, UK

(Received 1 October 2002 and in revised form 11 June 2003)

A numerical and analytical investigation is made into the response of a fluid when a two-dimensional structure is forced to move in a prescribed fashion. The structure is constructed in such a way that it supports a trapped mode at one particular frequency. The fluid motion is assumed to be small and the time-domain equations for linear water-wave theory are solved numerically. In addition, the asymptotic behaviour of the resulting velocity potential is determined analytically from the relationship between the time- and frequency-domain solutions. The trapping structure has two distinct surface-piercing elements and the trapped mode exhibits a vertical 'pumping' motion of the fluid between the elements. When the structure is forced to oscillate at the trapped-mode frequency an oscillation which grows in time but decays in space is observed. An oscillatory forcing at a frequency different from that of the trapped mode produces bounded oscillations at both the forcing and the trapped-mode frequency. A transient forcing also gives rise to a localized oscillation at the trapped-mode frequency which does not decay with time. Where possible, comparisons are made between the numerical and asymptotic solutions and good agreement is observed. The calculations described above are contrasted with the results from a similar forcing of a pair of semicircular cylinders which intersect the free surface at the same points as the trapping structure. For this second geometry no localized or unbounded oscillations are observed. The trapping structure is then given a sequence of perturbations which transform it into the two semicircular cylinders and the time-domain equations solved for a transient forcing of each structural geometry in the sequence. For small perturbations of the trapping structure, localized oscillations are produced which have a frequency close to that of the trapped mode but with amplitude that decays slowly with time. Estimates of the frequency and the rate of decay of the oscillation are made from the time-domain calculations. These values correspond to the real and imaginary parts of a pole in the complex force coefficient associated with a frequency-domain potential. An estimate of the position of this pole is obtained from calculations of the added mass and damping for the structure and shows good agreement with the time-domain results. Further time-domain calculations for a different trapping structure with more widely spaced elements show a number of interesting features. In particular, a transient forcing leads to persistent oscillations at two distinct frequencies, suggesting that there is either a second trapped mode, or a very lightly damped near-trapped mode. In addition a highly damped pumping mode is identified.

1. Introduction

Trapped water waves are free oscillations of an unbounded fluid with a free surface, for which the fluid motion is essentially confined to the vicinity of a fixed structure. Thus the energy of the motion is finite and there is no radiation of energy to infinity. Such modes are non-trivial solutions of the linearized water-wave problem in the frequency domain. They satisfy homogeneous boundary conditions and contain no waves in the far field (hence there is an absence of any forcing either from incident waves or from an imposed motion of the structure). The non-existence of a trapped-mode solution to the homogeneous problem at a particular frequency implies the uniqueness of the solution to a forcing problem at that frequency. Over a period of fifty years much work has gone into establishing uniqueness theorems for particular structural geometries (see for example John 1950 and Simon & Ursell 1984) but no general uniqueness proof has been found. The reason for this is now apparent as it has been discovered recently (McIver 1996) that trapped modes exist and may be supported at specific frequencies by certain 'trapping structures' with particular geometries. Surface-piercing and submerged trapping structures have been constructed in both the two- and three- dimensional water-wave problems (see McIver & Porter 2002 and the references therein).

The existence of a trapped mode at a particular frequency implies the non-uniqueness, or even non-existence, of the solution to the scattering or radiation problem at that frequency (McIver 1997). Furthermore the velocity potentials for certain forcing problems are singular at the trapped-mode frequency. These singularities in the potential manifest themselves as singular behaviour of hydrodynamic coefficients such as the added mass, and a detailed discussion of this and the implications for numerical calculations are given by Newman (1999) and McIver (2003). This paper is concerned mainly with the implications of the existence of trapped modes for the linearized water-wave problem in the time domain, but these connections with the frequency domain are also explored further.

Detailed analyses of particular time-domain water-wave problems are relatively rare. Exact solutions for the generation of waves by a moving paddle and by a moving vertical cylinder were obtained by Kennard (1949) and McIver (1994), respectively. The decay of the motion of a floating body was studied by Ursell (1964) and Maskell & Ursell (1970) for the vertical displacement of a half-immersed horizontal cylinder and by Smith (1982) for a rolling strip. On the other hand, many researchers have investigated the interaction between waves and structures in the time domain using numerical methods. Many of the methods have been developed for the nonlinear problem, although such methods are easily adapted to the linear problem. Recent papers on the forced vertical motion of a structure, which is investigated here, include those of Isaacson & Ng (1993) and Maiti & Sen (2001*b*).

The present work is concerned with the time-domain solution of the two-dimensional problem for the motion of an inviscid fluid around a structure that is constructed to support a trapped mode with a particular frequency of oscillation. Each 'trapping structure' has two distinct surface-piercing elements and most of the fluid motion associated with the trapped mode occurs between the two elements. To simplify matters, rather than allow the structure to respond freely to an initial disturbance, a variety of prescribed vertical motions are imposed, and a mixture of asymptotic and numerical methods is used to demonstrate how the existence of the trapped mode manifests itself. A typical scenario is as follows. Suppose that the structure is initially at rest and is then displaced in some prescribed way before being brought back to rest. In the linearized problem the fluid motion generated may

be thought of as an integral over components with all frequencies. The motions at frequencies other than the trapped-mode frequency ω_0 will die away as a result of wave radiation to infinity. However, a component of the motion at the trapped-mode frequency is not able to radiate energy to infinity and will persist with constant amplitude for all time, even though the structure itself is brought to rest. Other scenarios investigated here are the forced oscillation of the structure at the trapped-mode frequency ω_0, and the forced oscillation at a frequency $\sigma \neq \omega_0$.

The plan of the paper is as follows. The time domain problem for the forced vertical motion of a structure in water is formulated in § 2, the large-time asymptotics of the solution to this problem are described in § 3 (under the assumption that the structure supports a single trapped mode), and a numerical method for the solution of the time-domain problem is outlined in § 4. The first set of numerical results presented and discussed in § 5 is for a trapping structure that supports a trapped fluid motion between the two elements that is mainly a vertical or 'pumping' oscillation. The trapped mode is found to be excited by a variety of forcings and, where possible, comparison is made with the large-time asymptotics. In § 6 perturbations of a trapping structure, to structures that no longer support trapped modes, are discussed and it is demonstrated how the decay of a fluid motion around such structures can be described in terms of frequency-domain quantities. In § 7, computations are presented for a trapping structure made up of two more widely spaced elements for which the associated trapped mode has two free-surface nodes between the elements. It is found that there is an additional mode of fluid oscillation that is either a second trapped mode, or a very lightly damped near-trapped mode.

2. Formulation

Attention is restricted to two dimensions and Cartesian coordinates (x, z) are chosen with z directed vertically upwards and with the origin in the mean free surface. The fluid domain is bounded below by a flat rigid bed at $z = -h$ and extends to infinity in both horizontal directions. The fluid is assumed to be inviscid and incompressible and the motion to be irrotational so that it may be described by a velocity potential $\Phi(x, z, t)$ that is a solution of Laplace's equation

$$\nabla^2 \Phi = 0 \quad \text{in the fluid} \tag{2.1}$$

and also the bed condition

$$\frac{\partial \Phi}{\partial z} = 0 \quad \text{on} \quad z = -h. \tag{2.2}$$

For a structure Γ that is forced to heave with a vertical component of velocity $V(t)$, the boundary condition to be applied on Γ is

$$\frac{\partial \Phi}{\partial n} = V(t) n_z \tag{2.3}$$

where n is a coordinate measured normal to Γ and n_z is the z component of the unit normal. The free-surface elevation of the fluid $\eta(x, t)$ is related to Φ through the linearized free-surface conditions

$$\frac{\partial \Phi}{\partial t} = -g\eta \quad \text{on} \quad z = 0 \tag{2.4}$$

and

$$\frac{\partial \eta}{\partial t} = \frac{\partial \Phi}{\partial z} \quad \text{on} \quad z = 0. \tag{2.5}$$

The motion will be started from rest subject to the initial conditions

$$\Phi(x, 0, 0) = \frac{\partial \Phi}{\partial t}(x, 0, 0) = 0 \tag{2.6}$$

and for any fixed time

$$\nabla \Phi \to 0 \quad \text{as} \quad |x| \to \infty. \tag{2.7}$$

3. Asymptotic solution for large time

The solution of the time-domain problem (2.1)–(2.7) may be obtained formally with the use of the Laplace transform. The transform of the time-domain potential Φ is defined by

$$\widehat{\phi}(x, z, s) = \int_0^\infty \Phi(x, z, t)\, \mathrm{e}^{-st}\, \mathrm{d}t, \quad \mathrm{Re}\, s > 0 \tag{3.1}$$

and the inverse transform by

$$\Phi(x, z, t) = \frac{1}{2\pi \mathrm{i}} \int_{\gamma - \mathrm{i}\infty}^{\gamma + \mathrm{i}\infty} \widehat{\phi}(x, z, s)\, \mathrm{e}^{st}\, \mathrm{d}s \tag{3.2}$$

where, in the usual way, the real number γ is chosen to ensure that the contour of integration is taken to the right of any poles in the integrand. The Laplace transform of the velocity $V(t)$ is written $\widehat{v}(s)$. Introduction of $v(\omega) = \widehat{v}(-\mathrm{i}\omega)$ and $\phi(x, z, \omega)$, defined so that

$$\widehat{\phi}(x, z, -\mathrm{i}\omega) = v(\omega)\phi(x, z, \omega), \tag{3.3}$$

allows (3.2) to be rewritten as

$$\Phi(x, z, t) = \frac{1}{2\pi} \int_{-\infty}^{\infty} v(\omega)\phi(x, z, \omega)\, \mathrm{e}^{-\mathrm{i}\omega t}\, \mathrm{d}\omega. \tag{3.4}$$

From the properties $v(-\omega) = \overline{v}(\omega)$ and $\phi(x, z, -\omega) = \overline{\phi}(x, z, \omega)$ of the Fourier transform (the overbar denotes complex conjugate), (3.4) may be written alternatively as

$$\Phi(x, z, t) = \frac{1}{\pi} \mathrm{Re} \int_0^\infty v(\omega)\phi(x, z, \omega)\, \mathrm{e}^{-\mathrm{i}\omega t}\, \mathrm{d}\omega, \tag{3.5}$$

where the paths of integration in (3.4) and (3.5) are taken over any poles in the integrand.

When ω is real the function $\phi(x, z, \omega)$ is just the standard frequency-domain heave potential, as it is a solution of the Laplace equation which satisfies the body boundary condition

$$\frac{\partial \phi}{\partial n} = n_z \quad \text{on} \quad \Gamma, \tag{3.6}$$

the free-surface condition

$$\frac{\partial \phi}{\partial n} = \frac{\omega^2}{g}\phi \quad \text{on} \quad z = 0, \tag{3.7}$$

a radiation condition, and has zero normal derivative on $z = -h$. Causality means that $\Phi = 0$ for $t < 0$ and so there are no poles of ϕ in $\mathrm{Im}\, \omega > 0$. Any pole of ϕ on $\mathrm{Im}\, \omega = 0$ corresponds to a trapped mode for the particular structure Γ. It

will be assumed in the following asymptotic analysis that for each trapping structure Γ there is exactly one trapped mode so that there are two poles of ϕ at the real values $\omega = \pm\omega_0$, say. The assumption of a single trapped mode is consistent with the numerical results described in § 5. (The analysis can be extended in a straightforward way to include further trapped modes at other frequencies.) The trapped mode is described by a frequency-domain potential $\phi_0(x, z)$, which is a non-trivial solution of the homogeneous frequency-domain problem with $\omega = \omega_0$ and which satisfies $\phi_0 \to 0$ as $|x| \to \infty$.

In the time-domain problem the forcing velocity used has the form

$$V(t) = a\cos\sigma t + b\sin\sigma t + c\cos\omega_0 t + d\sin\omega_0 t + E(t), \tag{3.8}$$

where all the quantities in (3.8) are real, $\sigma > 0$, $\sigma \neq \omega_0$, and $E(t) \to 0$ as $t \to \infty$. This means that the motion of the body is totally prescribed and it is the response of the fluid that is of interest. The first two terms in (3.8) represent an oscillatory forcing at a frequency different from that of the trapped mode. The third and fourth terms represent a forcing at the trapped-mode frequency, and the final term represents a transient motion of the body. The effect of each of these types of forcing will be discussed in § 5.

The transform of the prescribed velocity in (3.8) is

$$v(\omega) = \frac{\mathrm{i}\omega a - \sigma b}{\omega^2 - \sigma^2} + \frac{\mathrm{i}\omega c - \omega_0 d}{\omega^2 - \omega_0^2} + e(\omega), \tag{3.9}$$

where

$$e(\omega) = \int_0^\infty E(t)\,\mathrm{e}^{\mathrm{i}\omega t}\,\mathrm{d}t, \tag{3.10}$$

and so $v(\omega)$ has simple poles at $\omega = \pm\sigma, \pm\omega_0$. Thus the integrand appearing in (3.5) has terms with a simple pole at $\omega = \sigma$ and, because there is a pole in ϕ at $\omega = \omega_0$, other terms with both simple and double poles at $\omega = \omega_0$. When the contour of integration is closed around the poles in the lower-half of the complex-ω plane it follows that

$$\Phi(x, z, t) \sim -2\,\mathrm{Re}\left\{\mathrm{i}\sum_{\text{residues}} v(\omega)\phi(x, z, \omega)\,\mathrm{e}^{-\mathrm{i}\omega t}\right\} \quad \text{as} \quad t \to \infty, \tag{3.11}$$

where the sum is taken over the residues of the poles of the integrand on the real axis in (3.5). (It may be shown that there is no contribution to Φ at leading order from either $\omega = 0$ or $\omega \to \infty$.)

It is shown in the Appendix that the heave potential has the form

$$\phi(x, z, \omega) = \frac{gA\phi_0(x, z)}{\omega^2 - \omega_0^2} + \phi_1(x, z) + O(\omega - \omega_0) \quad \text{as} \quad \omega \to \omega_0 \tag{3.12}$$

where

$$A = \frac{-\displaystyle\int_\Gamma \phi_0(\xi, \eta)\, n_\eta\,\mathrm{d}s}{\displaystyle\int_F [\phi_0(\xi, 0)]^2\,\mathrm{d}\xi} = \frac{-\displaystyle\int_{-\infty}^{\infty} \phi_0(\xi, -h)\,\mathrm{d}\xi}{\displaystyle\int_F [\phi_0(\xi, 0)]^2\,\mathrm{d}\xi}, \tag{3.13}$$

s is arclength, F denotes the mean free surface and ϕ_1 satisfies Laplace's equation, the body boundary condition (3.6), a radiation condition, a forced free-surface boundary

condition

$$\frac{\omega_0^2}{g}\phi_1 - \frac{\partial \phi_1}{\partial z} = -A\phi_0(x,0) \quad \text{on} \quad z = 0, \tag{3.14}$$

and has zero normal derivative on $z = -h$. The Fredholm Alternative may be used to show that ϕ_1 exists, and uniqueness is ensured by the requirement that

$$\int_F \phi_1(x,0)\,\phi_0(x,0)\,\mathrm{d}x = 0. \tag{3.15}$$

The pole structure in ϕ and v given by equations (3.9) and (3.12) allows the required residues in (3.11) to be calculated and the asymptotic form of Φ as $t \to \infty$ to be found. The free-surface elevation then follows from (2.4) and, after some manipulation, it is found that

$$\begin{aligned}\eta(x,t) \sim A\phi_0(x,0)\Bigg[&\frac{1}{2\omega_0}(d\omega_0 t \sin\omega_0 t + c\omega_0 t\cos\omega_0 t + c\sin\omega_0 t)\\ &+ \frac{1}{\omega_0^2 - \sigma^2}(a\omega_0\sin\omega_0 t - b\sigma\cos\omega_0 t) + \int_0^\infty E(\tau)\cos\omega_0(t-\tau)\,\mathrm{d}\tau\Bigg]\\ &- \frac{1}{g}\,\mathrm{Re}\left[\sigma(b - \mathrm{i}a)\phi(x,0,\sigma)\,\mathrm{e}^{-\mathrm{i}\sigma t} + \omega_0(d - \mathrm{i}c)\phi_1(x,0)\,\mathrm{e}^{-\mathrm{i}\omega_0 t}\right] \quad \text{as} \quad t \to \infty.\end{aligned} \tag{3.16}$$

The first group of terms in (3.16), with the trapped-mode potential ϕ_0 as a factor, corresponds to excitation of the trapped mode. The forcing at the trapped-mode frequency ω_0 through the terms involving c and d gives a resonance and there are components of the free-surface oscillation which have an amplitude that grows linearly with time. Because $\phi_0 \to 0$ as $|x| \to \infty$, at any particular t the resonance will not be observed in the far field, but there is a non-decaying radiated wave at the trapped-mode frequency given by the term in ϕ_1. The transient $E(t)$ in the forcing velocity excites a non-resonant trapped mode. The forcing at a frequency $\sigma \neq \omega_0$, identified by the terms involving a and b, excites a steady oscillation of the trapped mode which will be localized to the vicinity of the structure and also generates a radiated wave at frequency σ through the heave potential $\phi(x,z,\sigma)$ at that frequency. In § 5 these three types of forcing are discussed separately.

4. Numerical method

In § 5 and § 7 numerical solutions of the initial-value problem (2.1)–(2.7) will be presented. The numerical method is an adaptation to this linear problem of that described by Maiti & Sen (2001*a*, *b*) for the solution of nonlinear initial-value problems.

For the purposes of the numerical calculations the problem (2.1)–(2.7) was made non-dimensional by scaling all lengths by the depth h and time by $\sqrt{h/g}$ (which is equivalent to choosing $g = h = 1$). With these scalings the only changes are to the sea-bed and the dynamic free-surface condition (2.2) and (2.4) in which h and g should be set equal to one. Throughout this section all variables will be used in their non-dimensional form.

The initial-value problem (2.1)–(2.7) is defined on a spatial domain that extends to infinity in both horizontal directions. For computational purposes it is necessary to truncate the domain to one of finite extent and Maiti & Sen (2001*a*, *b*) achieved this

by introducing two rigid vertical walls. However, it is better to apply a scheme that reduces reflections from the artificial boundaries. An effective scheme is described by Clément (1996) in which rigid pistons at $x = \pm L$, say, are combined with two damping zones of width G occupying $L - G < |x| < L$; the pistons are most effective at absorbing long waves and the damping zones are most effective with short waves. For all of the computations reported here $L = 15$ and $G = 5$.

The piston boundary condition proposed by Clément (1996) is

$$\frac{\partial \Phi}{\partial x}(\pm L, z, t) = \mp \int_{-1}^{0} \frac{\partial \Phi}{\partial t}(\pm L, \zeta, t)\, \mathrm{d}\zeta, \quad -1 < z < 0, \tag{4.1}$$

so that each piston is rigid and makes horizontal movements in response to the fluid pressure on its surface. For long waves, in which the fluid motion is independent of the depth, (4.1) reduces to

$$\frac{\partial \Phi}{\partial x} = \mp \frac{\partial \Phi}{\partial t} \quad \text{at} \quad x \pm L, \tag{4.2}$$

which are the Sommerfeld conditions for waves with speed one (equivalent to the long-wave speed $\sqrt{gh}$ when (4.2) is expressed in terms of dimensional quantities). Clément (1996) does not describe how the conditions (4.1) are implemented within his code. In the numerical code used here the piston conditions are applied by writing (4.1) in the form

$$\frac{\mathrm{d}q_{\pm}}{\mathrm{d}t} = -u_{\pm}(t) \tag{4.3}$$

where $u_{\pm}$ is the velocity of the piston at $x = \pm L$ measured in the direction out of the fluid domain, and

$$q_{\pm}(t) = \int_{-1}^{0} \Phi(\pm L, \zeta, t)\, \mathrm{d}\zeta. \tag{4.4}$$

Equation (4.3) is used to increment $q_{\pm}$ once $u_{\pm}$ have been determined in the manner outlined below.

The damping zones are introduced by modifying the non-dimensional form of the dynamic free-surface boundary condition (2.4) to be

$$\frac{\partial \Phi}{\partial t} = -\eta - \nu(x) \frac{\partial \Phi}{\partial z} \quad \text{on} \quad z = 0 \tag{4.5}$$

where $\nu(x) = 0$ for $|x| \leqslant L - G$, and $\nu(x) > 0$ for $L - G < |x| < L$ to ensure that the additional term dissipates energy within the damping zone. As suggested by Clément (1996), the form

$$\nu(x) = \frac{0.2}{G^3} \left[3G(|x| - L + G)^2 - 2(|x| - L + G)^3 \right] \tag{4.6}$$

is adopted which, in particular, ensures that $\nu(\pm(L-G)) = \nu'(\pm(L-G)) = \nu'(\pm L) = 0$.

The computational domain D is illustrated schematically in figure 1. There are two surface-piercing structures denoted by S_1 and S_2 and three portions of the free surface denoted by F_1, F_2 and F_3. The bed at $z = -1$ is denoted by B and the pistons at $x = \pm L$ by $P_{\pm}$. An application of Green's theorem over the whole of the domain boundary ∂D to the velocity potential Φ and a Green's function G gives

$$\alpha(p)\Phi(p) = \int_{\partial D} \left[\Phi(q) \frac{\partial G}{\partial n_q}(p, q) - G(p, q) \frac{\partial \Phi}{\partial n_q}(q) \right] \mathrm{d}s_q, \quad p \in \partial D, \tag{4.7}$$

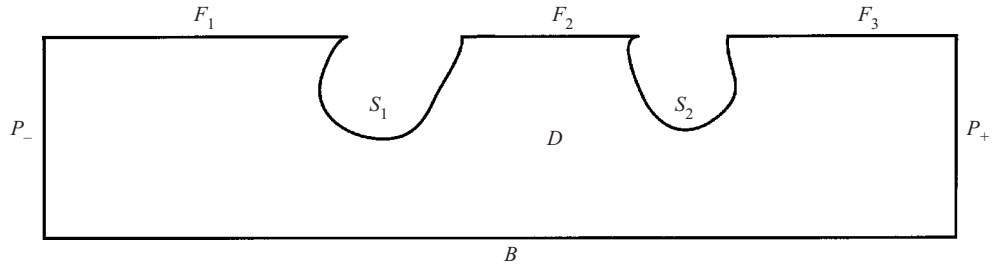

FIGURE 1. The computational domain.

where the normal derivatives denoted using n_q are directed out of the domain, $\alpha(p)$ is the interior angle at p, and

$$G \sim \frac{1}{2\pi} \log R_{pq} \tag{4.8}$$

as the distance R_{pq} between p and q tends to zero. The Green's function G is chosen to be a simple source together with its image in the bed B so that the integration over B in (4.7) vanishes.

At the beginning of a time step $\partial\Phi/\partial n$ is known on $S = S_1 \cup S_2$ through (2.3) and it is assumed that Φ and η are given on $F = F_1 \cup F_2 \cup F_3$ and $q_\pm$ are given on $P_\pm$ (they are all zero initially). The unknowns are the piston velocities $u_\pm$, Φ on both $P_\pm$ and S, and $\partial\Phi/\partial n$ on F. The numerical scheme used to determine approximations to these unknowns is as follows. Nodes are distributed over the boundary $\partial D \backslash B$ and the variations in Φ, $\partial\Phi/\partial n$, and the geometry, are described in terms of cubic splines. A cosine spacing was used to distribute the nodes on each portion of the boundary so that they are more concentrated near corner points. The details of the representation in terms of cubic splines are given by Sen (1995) and are not repeated here. The cubic-spline representation is used to discretize (4.4) and (4.7) in terms of the nodal values of Φ and $\partial\Phi/\partial n$ (including $u_\pm$) and then these equations, augmented by continuity of Φ at all intersections of the boundary portions, can be used to determine the unknowns listed above. It is worthy of note that in this linear problem the coefficient matrix obtained in the discretization of (4.7) does not change with time and need only be computed once. To proceed to the next time step the conditions (2.5) and (4.5) are used to increment η and Φ on the free surface, and (4.3) is used to increment $q_\pm$. The time stepping was carried out using the fourth-order Runge–Kutta method.

It is well-known that when boundary integral equations are solved for normal derivatives significant errors can arise near any corners. An important feature of the solution of (4.7) by the method used here is the control of such errors in the values of $\partial\Phi/\partial n$. The cubic representation of the variation in the unknowns, the distribution of the nodes using cosine spacing, and the imposition of continuity of velocity at the corners (see Sen 1995) all help keep these errors within acceptable bounds. This is particularly important when time-stepping is involved as any errors in the solution of the integral equation will accumulate over time.

5. Results for a pumping-mode trapping structure

The first set of results described here concern the forced heave motion of the trapping structure shown in figure 2. Following the inverse procedure given by McIver (1996), applied here in finite depth, this structure was obtained from the flow

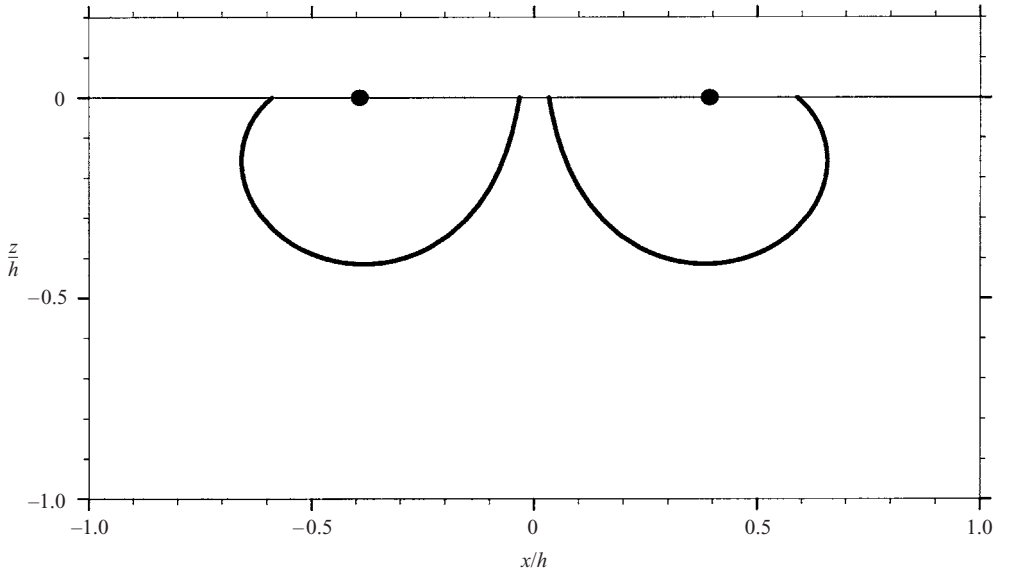

FIGURE 2. A trapping structure for source positions $x_0 = \pm\pi h/8$ corresponding to $kh = 4$. The positions of the sources are marked by filled circles.

field due to two oscillatory sources placed at $x_0/h = \pm\pi/8$. For a trapped mode it is required that there are no waves as $|x| \to \infty$ and the construction ensures this provided the oscillation frequency $\omega_0 = \sqrt{(4\tanh 4)g/h} \approx 1.99933\sqrt{g/h}$; this corresponds to $kh = 4$ where k is the wavenumber of free waves of frequency ω_0 in water of depth h. A trapping structure is obtained from any streamlines of the flow that separate the singular points of the flow field from infinity. In the case shown in figure 2 the particular streamlines chosen are those that emanate from the free surface at $x/h = \pm 3\pi/16$. For the above choices of source positions and frequency, the fluid motion between the structural elements is a 'pumping' mode without nodes.

In figures 3, 5, 6, 8 and 11, the free-surface elevation $\eta(x, t)$ is given as a function of time for two particular values of x; in part (a) of each of these figures $x = 0$, the mid-point between the two structural elements, and in part (b) $x/h \approx 5$, which for convenience is referred to as the far field. The times are scaled by $T = \sqrt{h/g}$.

Figure 3 gives the free-surface elevation as a function of time resulting from a displacement of the trapping structure given by

$$S(t) = \alpha h(t/T)^3 \,\mathrm{e}^{-t/T} \tag{5.1}$$

for some arbitrary constant $\alpha \ll 1$ (the velocity $V(t) = S'(t)$ so that $a = b = c = d = 0$ in (3.8)). In this case the structure returns to its equilibrium position as $t \to \infty$ in a prescribed fashion. (It is worth noting that this scenario is not equivalent to giving the structure an initial displacement and then releasing it, an example of which is discussed by Maskell & Ursell 1970. In that case the coupled motion of the body and fluid would need to be found.) The factor of t^3 is included to ensure that there is no discontinuity in either the velocity or the acceleration as the structure begins to move. Between the structures the asymptotic trapped mode is quickly established and, in figure 3(a), a steady oscillation of the free surface is observed as the trapped mode does not give any radiation of energy to infinity. This trapped mode decays rapidly

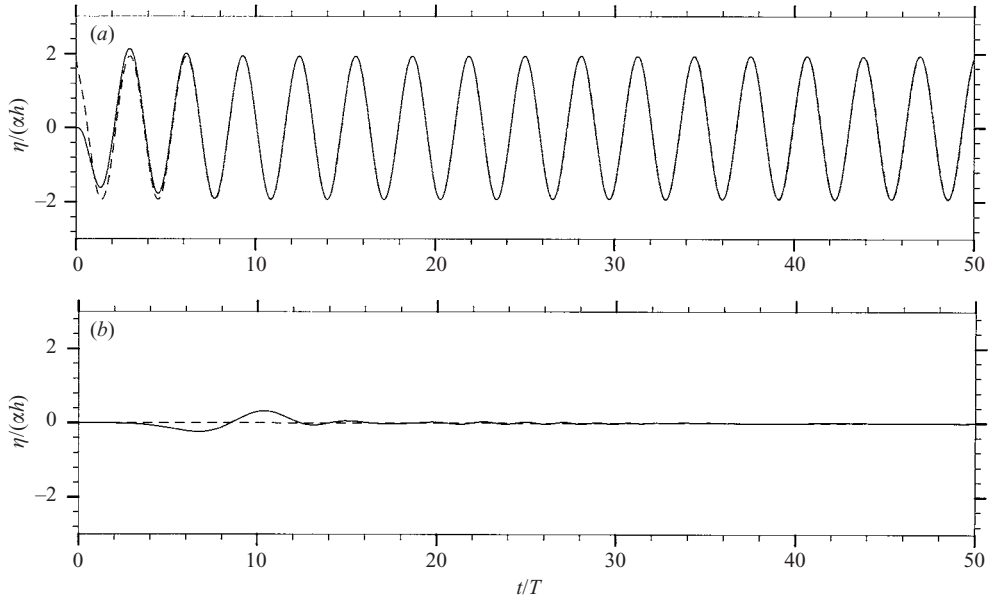

FIGURE 3. Free-surface elevation η as a function of time t for a trapping structure after a transient disturbance: (*a*) mid-point, (*b*) far field. The figures compare the numerical solution (———) with the asymptotic solution (– – – –).

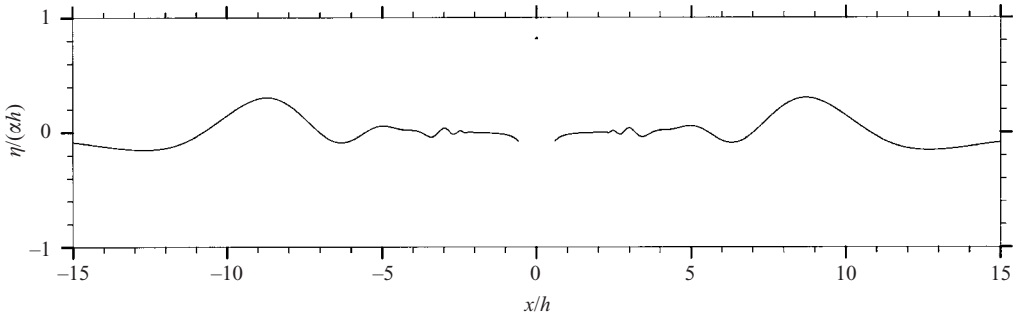

FIGURE 4. Free-surface elevation η at time $t = 15T$ as a function of x for a trapping structure after a transient disturbance.

away from the structural elements and hence at the far-field point, figure 3(*b*), the motion dies away after the waves arising from the initial disturbance have propagated through. The spatial variation of the free surface at time $t = 15T$ is shown in figure 4. The initial disturbance that radiates away is clearly seen. The small length of free surface between the structures (the trapped mode) has an elevation $\eta \approx 0.83\alpha h$ at this time and appears as a dot in the figure.

The results for figure 3 can be contrasted with those shown in figure 5 for two half-immersed circular cylinders whose free-surface intersections coincide with those of the trapping structure shown in figure 2. There is no general uniqueness theorem for this geometry to rule out the existence of trapped modes, although Linton & Kuznetsov (1997) do show that, for a fixed configuration of cylinders, there are certain frequency bands which are free of trapped modes. However, the numerical

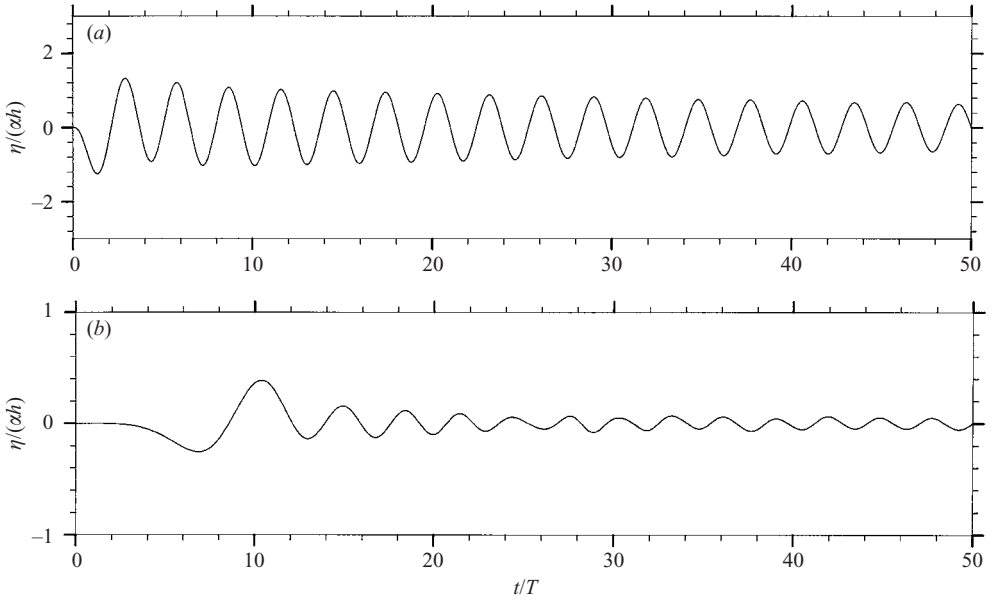

FIGURE 5. Free-surface elevation η as a function of time t for two half-immersed circular cylinders after a transient disturbance: (*a*) mid-point, (*b*) far field.

results shown in figure 5, for the two cylinders given the vertical displacement (5.1), do suggest that for this configuration of cylinders there are no trapped modes at any frequency that can be resolved by the discretization of the equations because, in contrast to figure 3(*a*), the numerical results of figure 5(*b*) indicate that there is no steady oscillation established between the cylinders (the discrete Fourier transform of this time signal also shows only a single peak frequency). The initial disturbance does set up a fluid oscillation between the cylinders but this decays slowly due to wave radiation, and this continual process of wave radiation to the far field can be seen in figure 5(*b*). The decay of fluid oscillations generated in this way and their frequencies of oscillation are discussed further in § 6.

Figures 6–8 give results for the trapping structure of figure 2 when it is forced to oscillate vertically with a velocity

$$V(t) = \begin{cases} \frac{1}{2}(1 - \cos(\pi t/t_m))\alpha h\omega \cos \omega t, & 0 \leqslant t < t_m, \\ \alpha h\omega \cos \omega t, & t \geqslant t_m, \end{cases} \tag{5.2}$$

which for $t \geqslant t_m$ corresponds to a displacement $S(t) = \alpha h \sin \omega t$. The additional factor in the definition of $V(t)$ for $0 \leqslant t < t_m$ is included to ensure that there are no discontinuities in velocity and acceleration at $t = 0$ and $t = t_m$. For the calculations reported here the choice $t_m = 4T$ was made.

The results of figures 6 and 7 are for an oscillation frequency $\omega = \omega_0$, the trapped-mode frequency (so that $a = b = d = E(t) = 0$ in (3.8)). This is the resonant case and the leading-order asymptotics as $t \to \infty$ in (3.16) involve an oscillation at the frequency ω_0 with an amplitude that grows linearly with time t. This oscillation involves the trapped-mode potential which decays to zero as $|x| \to \infty$ and, hence, the growing oscillation is observed between the structures (figure 6*a*) but not in the far field (figure 6*b*). A forced oscillation of the structure at the trapped-mode frequency

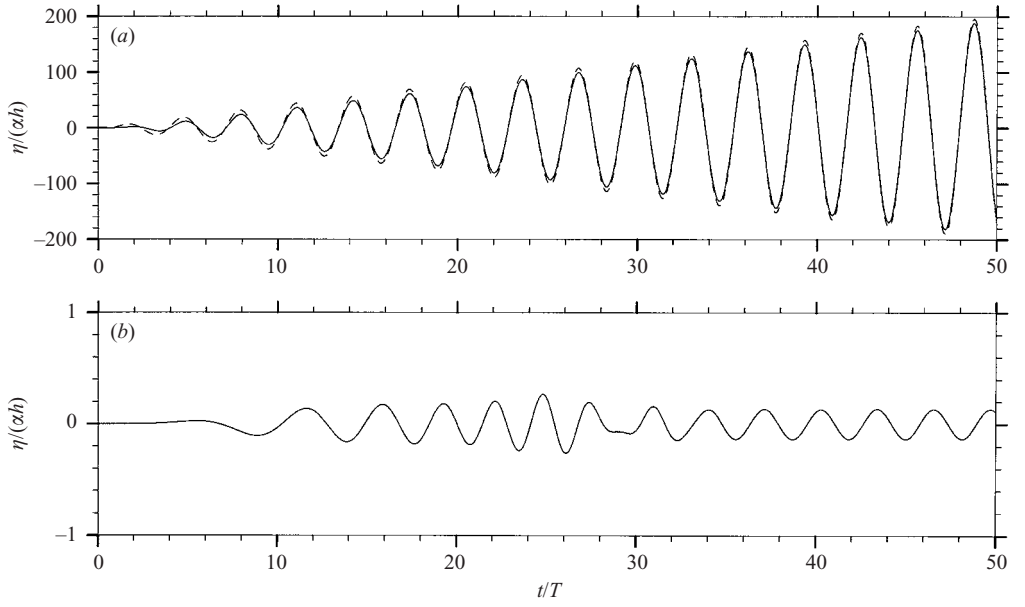

FIGURE 6. Free-surface elevation η as a function of time t for a trapping structure forced to oscillate at the trapped-mode frequency ω_0: (*a*) mid-point, (*b*) far field. In (*a*) the numerical solution (———) is compared with the leading-order asymptotic solution (– – – –) whilst (*b*) shows only the numerical solution.

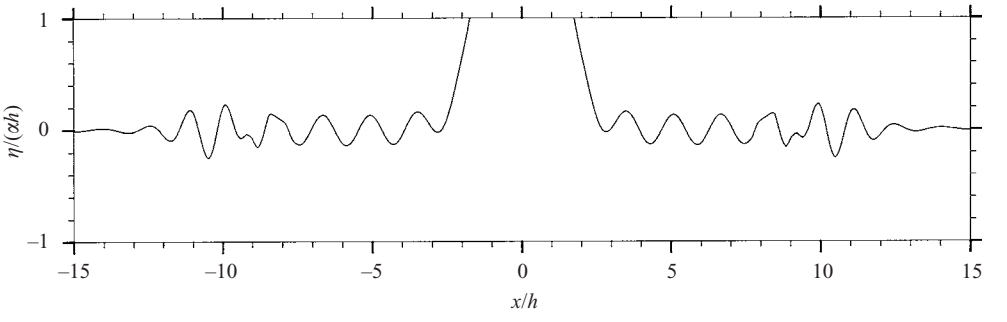

FIGURE 7. Free-surface elevation η at time $t = 50T$ as a function of x for a trapping structure forced to oscillate at the trapped-mode frequency ω_0.

does involve radiation of waves to the far field, through the term in (3.16) that involves ϕ_1, and this can be seen in figure 6(*b*) after about $t = 32T$. The features before this time arise from the transient effects associated with the initial condition. Only the terms in the asymptotic solution (3.16) that have linear growth in t are easily computed so comparisons in figure 6 are restricted to these terms.

For this resonant case, the free-surface elevation η at time $t = 50T$ is plotted against x in figure 7. The vertical scale is truncated in order to show clearly the wave motion on the outer portions of the free surface. Adjacent to the structure there is a large-amplitude standing-wave motion, that at this time extends up to $\eta \approx 17\alpha h$, due to the resonant trapped mode. As this mode decays with increasing $|x|$ the wave radiation at frequency ω_0 due to the term ϕ_1 in (3.16) becomes apparent, although at this time it does not fully extend to the edge of the damping zone at $|x| = 10h$.

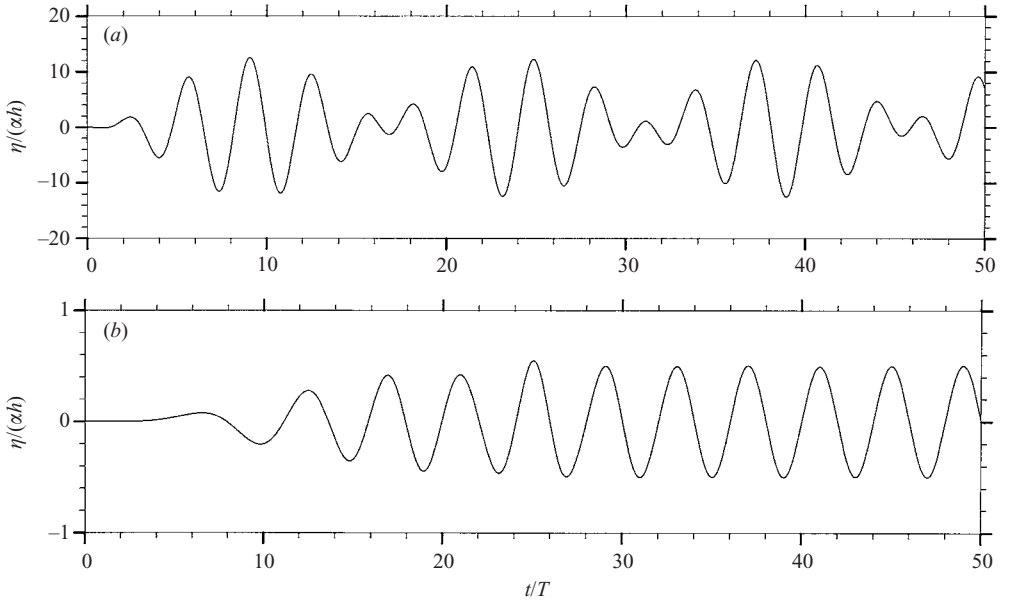

FIGURE 8. Free-surface elevation η as a function of time t for a trapping structure forced to oscillate at a frequency $\sigma \neq \omega_0$: (*a*) mid-point, (*b*) far field.

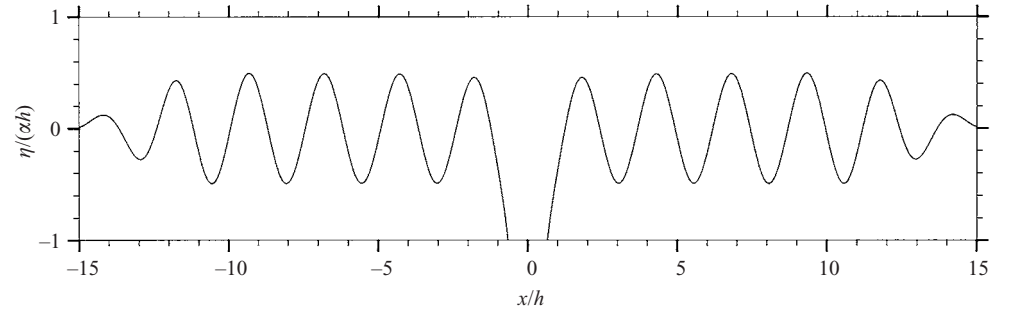

FIGURE 9. Free-surface elevation η at time $t = 100T$ as a function of x for a trapping structure forced to oscillate at a frequency $\sigma \neq \omega_0$.

The results of figures 8 and 9 are for an oscillation frequency $\omega = \sigma \neq \omega_0$, where σ has been arbitrarily chosen as $\pi/2T$ (so that $b = c = d = E(t) = 0$ in (3.8)). For large time the fluid response now contains two oscillatory components, one at the forcing frequency σ and one at the trapped-mode frequency ω_0. The σ component of the asymptotic solution is just the standard frequency-domain solution which involves wave radiation to infinity. The ω_0 component is a trapped mode that decays with distance from the structure. Hence, the free-surface elevation in figure 8(*a*), measured between the structures, contains significant contributions from both frequencies. However, in the far field, shown in figure 8(*b*), the wave radiation with frequency σ is dominant. It is apparent that, for a structure that supports a trapped mode, almost any initial condition will lead to persistent fluid oscillations at the trapped-mode frequency ω_0 in addition to oscillations at the forcing frequency σ.

The spatial variation of the free-surface elevation η at time $t = 20T$ is shown in figure 9. Again, the vertical scale is truncated in order to show the wave motion on

the outer portions of the free surface. By this time wave radiation at the frequency σ is well established, and the attenuation of the wave train due to the damping zone in $10h < |x| < 15h$ and the pistons at $|x| = 15h$ is clearly apparent.

6. Decay of fluid oscillations

Of some practical significance is the sensitivity of the results to geometrical perturbations of a trapping structure away from a shape that supports trapped modes. It has already been seen in figure 5 for a configuration of two half-immersed circular cylinders, which (probably) does not support trapped modes, that an oscillation between the two structures is readily excited but that its amplitude decays with time. Here the perturbation of a trapping structure into two-half immersed cylinders is investigated in detail. In particular, an investigation is made of the effects of such perturbations on the decay rate of fluid oscillations in the time domain or, equivalently, on the position of a simple pole in the frequency-domain potential.

The structural perturbations were made in the following way. The surface of the right-hand element of a trapping structure is denoted by $r = f_t(\theta)$ (see, for example, figure 2) and the surface of the right-hand semicircle in a pair by $r = f_c(\theta)$, where r and θ are polar coordinates with origin at the centre of the free-surface intersection, $0 \leqslant \theta \leqslant \pi$ and $f_c(0) = f_t(0)$ and $f_c(\pi) = f_t(\pi)$. A family of structures, all having the same intersection with the free surface, is given by

$$r = \chi f_t(\theta) + (1 - \chi) f_c(\theta) \tag{6.1}$$

where χ is a real number in the interval $[0, 1]$. Clearly, $\chi = 1$ recovers the trapping structure and $\chi = 0$ the semicircle. The left-hand element of a pair of structures is obtained by reflection in $x = 0$.

As already noted in § 3, the existence of a symmetric trapped mode for a given structure implies that in the complex frequency domain the heave potential has a pole on the real axis. As the structure is perturbed away from one that supports a trapped mode the pole moves into the lower half-plane and becomes a so-called 'complex resonance' or 'scattering frequency'. Such frequencies have been investigated in the context of acoustic-wave scattering by Lenoir, Vullierme-Ledard & Hazard (1992) and the generation of complex resonances due to geometric perturbations of a trapping structure in an acoustic waveguide has been studied analytically by Aslanyan, Parnovski & Vassiliev (2000). In the context of water-wave problems the effect of the complex resonances on the hydrodynamic coefficients of 'near-trapping' structures has been studied by Linton & Evans (1992), Martin & Farina (1997) and Newman (1999).

Suppose that the frequency-domain heave potential $\phi(x, z, \omega)$ for a structure has a pole at $\omega = \omega_0 - \mathrm{i}\epsilon$ with $\omega_0 > 0$ and $\epsilon \geqslant 0$, so that

$$\phi(x, z, \omega) \sim \frac{\varphi_0(x, z)}{\omega - (\omega_0 - \mathrm{i}\epsilon)} \quad \text{as} \quad \omega \to \omega_0 - \mathrm{i}\epsilon. \tag{6.2}$$

It is assumed here that any other poles that may exist are sufficiently far from the real-ω-axis to be negligible in the determination of the large-time asymptotics. Here only a transient forcing $V(t) = E(t)$ is considered so that the Fourier transform $v(\omega)$ of the forcing velocity has no poles. The contribution to the large-time asymptotics from the pole in ϕ can be obtained from (3.5) by closing the contour of integration around the pole in the fourth quadrant. The detailed analytical structure of $\phi(x, z, \omega)$ in the complex-ω-plane is unknown so that the contribution to the asymptotics from

	Time		Frequency	
χ	ω_0	ϵ	ω_0	ϵ
0	2.17	0.0124	2.17	0.0127
0.2	2.14	0.0082	2.14	0.0083
0.4	2.11	0.0046	2.11	0.0046
0.6	2.08	0.0020	2.08	0.0020
0.8	2.04	0.0005	2.04	0.0005
1.0	2.00	0.0000		

TABLE 1. Location of complex resonances for a perturbed trapping structure obtained from the time- and frequency-domain calculations.

the remaining integral cannot be calculated. However it may be shown that Φ does not contain any algebraic decay with time, in contrast to the transient vertical motion of an unconstrained cylinder in infinite depth fluid (see Ursell 1964). Such algebraic decay would arise in (3.5) as a result of the behaviour of ϕ as $\omega \to 0$. It can be deduced from Bai (1977) (see also McIver & Linton 1991) that

$$\phi(x, z, \omega) \sim \frac{1}{\mathrm{i}\omega} \sum_{n=0}^{\infty} (\mathrm{i}\omega)^n \phi_n(x, z) \quad \text{as} \quad \omega \to 0, \tag{6.3}$$

where each ϕ_n is real valued, and for the forcing (5.1) the velocity $V(t)$ has the Fourier transform $v(\omega) = -6\mathrm{i}\omega/(1 - \mathrm{i}\omega)^4$. Repeated integration by parts in (3.5) then shows that $\Phi(x, z, t)$ contains no powers of t in its asymptotic expansion as $t \to \infty$. (This is true for all forcings $V(t)$ such that

$$v(\omega) \sim \sum_{n=1}^{\infty} c_n (\mathrm{i}\omega)^n \quad \text{as} \quad \omega \to 0, \tag{6.4}$$

where the c_n are real, provided that $v(\omega)\phi(x, z, \omega) = o(1)$ as $\omega \to \infty$.) This result and the numerical computations presented here suggest that the leading-order contribution to the large-time behaviour does arise from the residue at the pole so that

$$\Phi(x, z, t) \sim -2 \operatorname{Re} \left\{ \mathrm{i} v(\omega_0) \varphi_0(x, z) \, \mathrm{e}^{-\mathrm{i}\omega_0 t} \right\} \mathrm{e}^{-\epsilon t} \quad \text{as} \quad t \to \infty. \tag{6.5}$$

In general this is a decaying oscillation but when the structure supports a trapped mode, so that $\epsilon = 0$, then the oscillation persists for all time.

The values of ω_0 and ϵ may be estimated from the results of a time-domain calculation (like that in figure 5) as follows. First, the times of the local maxima in the free-surface elevation were obtained (the first five maxima were omitted to reduce the effects of the initial transient). The frequency ω_0 was found from the average of the times between successive maxima. The decay constant ϵ was found from the gradient of a straight line fitted to the logarithms of the free-surface maxima as a function of time. The results of these time-domain calculations are given in table 1 for a series of structures parameterized by χ, which was introduced in equation (6.1).

The location of a complex resonance may also be calculated from the frequency-domain problem and a direct method is described by Hazard & Lenoir (1993). However, provided the pole is close to the real axis, a good estimate of the location of a complex resonance may be obtained from a standard frequency-domain code

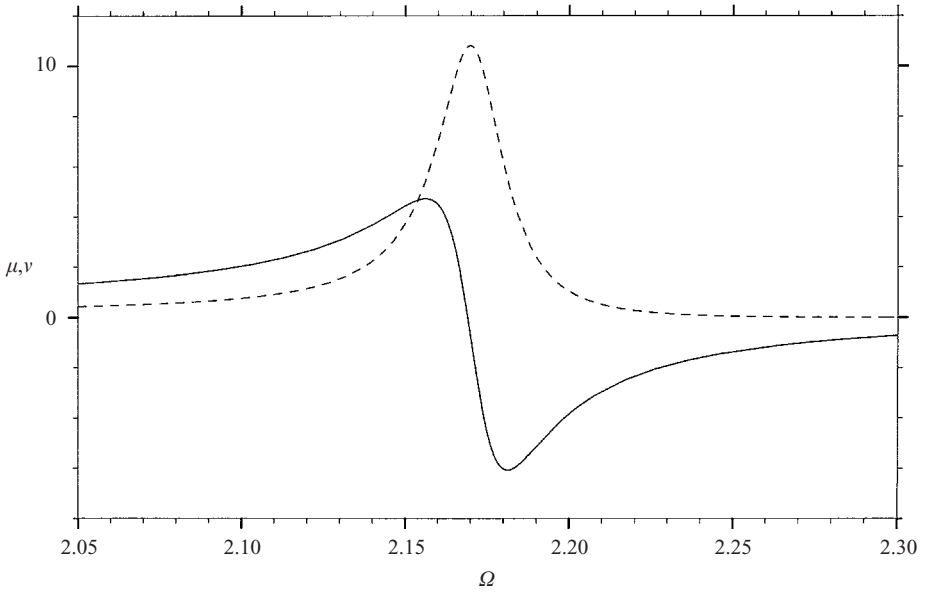

FIGURE 10. Non-dimensional added mass μ (———) and damping ν (– – – –) as a function of non-dimensional frequency $\Omega = \omega\sqrt{g/h}$ for two half-immersed circular cylinders.

for the calculation of hydrodynamic coefficients at real frequencies. If there is a pole in the heave potential at $\omega = \omega_0 = \omega_0 - \mathrm{i}\epsilon$, then there will be a corresponding pole in the complex force coefficient so that

$$\mu + \mathrm{i}\nu \sim \frac{-\mathscr{A}}{\omega - (\omega_0 - \mathrm{i}\epsilon)} \quad \text{as} \quad \omega \to \omega_0 - \mathrm{i}\epsilon. \tag{6.6}$$

Here μ and ν are respectively the non-dimensional added-mass and damping coefficients and $\mathscr{A}$ is a real, positive constant which ensures that $\nu > 0$ (something that is required from energy considerations). According to the asymptotic form of $\mu + \mathrm{i}\nu$ in equation (6.6), on the real-ω-axis there is a local maximum in ν at $\omega = \omega_0$ and a local maximum and a local minimum in μ at respectively $\omega = \omega_0 \mp \epsilon$. Typical added mass and damping curves near a resonant frequency are shown in figure 10 (the structural geometry is the pair of semicircles) and the features noted above are clearly observed. It is a simple matter to obtain the positions of the local extrema and hence compute approximate values for ω_0 and ϵ; the results of such calculations are shown in table 1. All of the frequency-domain calculations shown in table 1 were made using a boundary-element method with thirty panels on each structure in a pair and with additional panelling of the interior free surfaces to remove irregular frequencies. It is clear from table 1 that, for these near-resonant situations, an important aspect of the behaviour in the time domain is readily predicted by examination of standard frequency-domain calculations.

7. Results for a sloshing-mode trapping structure

The results presented so far have been related to a trapping structure for which the trapped-mode fluid motion between the elements of the structure is a pumping

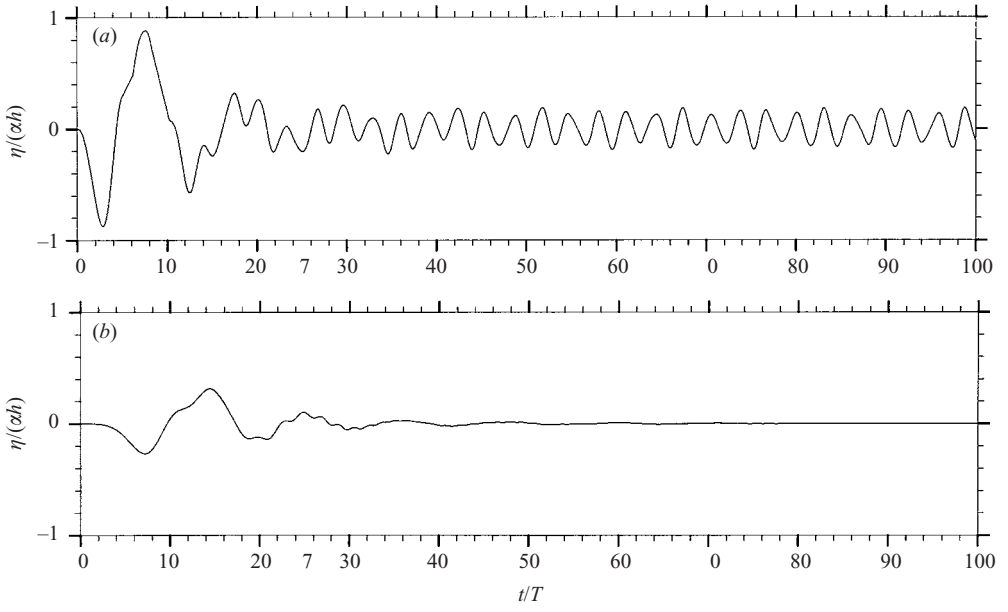

FIGURE 11. Free-surface elevation η as a function of time t for a sloshing-mode trapping structure after a transient disturbance: (a) mid-point, (b) far field.

motion without free-surface nodes. The method of construction used to generate this structure may be used to generate other trapping structures for which the fluid motion between the structures does have nodes, and one such example is studied here. Oscillatory sources are placed at $x_0/h = \pm 3\pi/8$ and, as before, waves are eliminated at infinity provided that the oscillation frequency $\omega_0 = \sqrt{(4 \tanh 4)g/h}$. It should be emphasized that the construction only guarantees the existence of a single trapped mode and it has frequency of oscillation ω_0. For the computations reported here the particular trapping structure is formed from the streamlines that emanate from the free surface at $x/h = \pm 9\pi/16$. The appearance of the two elements of the trapping structure is similar to those shown in figure 2, but they are more widely spaced. The trapped mode is symmetric about $x = 0$ and has two free-surface nodes between the structural elements; to distinguish this from the pumping mode discussed earlier it will be referred to as a 'sloshing' mode.

Time-domain results for the sloshing-mode trapping structure, with a transient forcing in the form of equation (5.1), are given in figures 11 and 12. Based on the results presented in § 5, it might have been expected that the motion between the two structural elements would settle to an oscillation at the trapped-mode frequency. However, from figure 11(a) this is clearly not the case even when the far-field plot figure 11(b) indicates that there is very little, or no, radiation. The snapshot at time $t = 98T$ shown in figure 12(b) confirms that the fluid motion contains components other than the constructed trapped mode because, at this particular time, there are four zero crossings of the mean water level instead of the two found in the constructed trapped mode. It seems that, in addition to the trapped mode that has been constructed at $\Omega = \omega_0/\sqrt{g/h} \approx 2.0$, there is a second mode that is either trapped or radiates very little energy.

The oscillation frequency of this second mode is estimated from the discrete Fourier transform (Press *et al.* 1992, § 12.1) of the time signal in figure 11(a), continued to

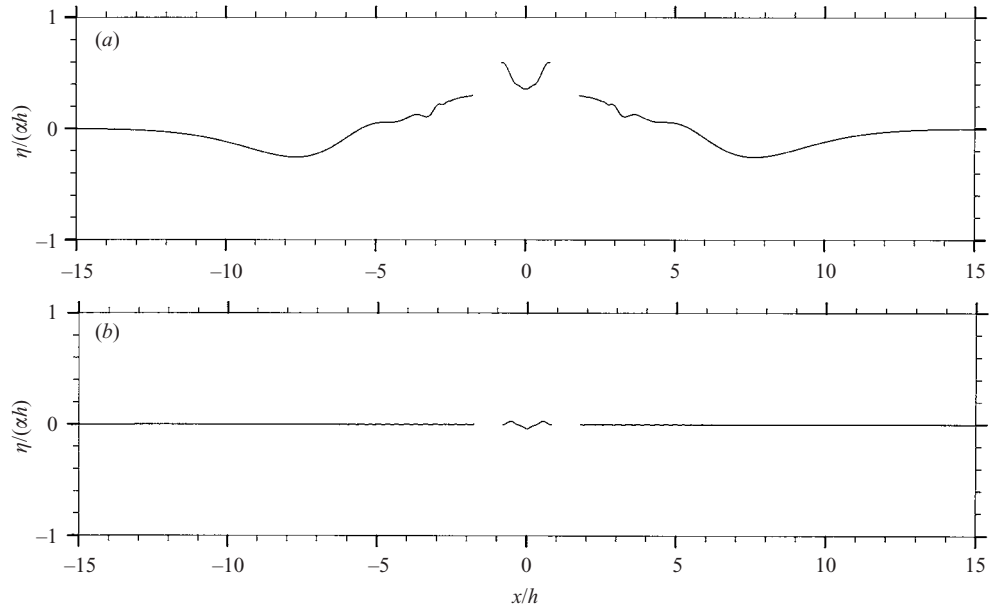

FIGURE 12. Free-surface elevation η at times (*a*) $t = 9T$ and (*b*) $t = 98T$ as a function of x for a sloshing-mode trapping structure after a transient disturbance.

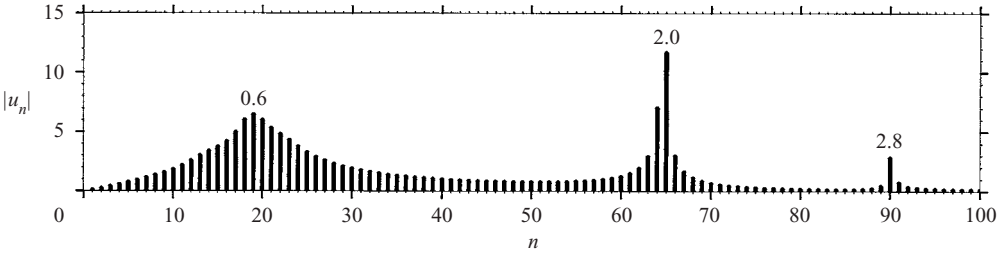

FIGURE 13. Discrete Fourier transform of the free-surface elevation shown in figure 11(*a*). Here $|u_n|$ is $N^{-1/2}$ times the amplitude of the Fourier component with index n, where N is the number of samples in the signal, and the numbers within the plot are the non-dimensional frequencies $\Omega = \omega/\sqrt{g/h}$ corresponding to the peaks at $n = 19, 65$ and 90.

$t = 200T$, and this is shown in figure 13. The index n used in that figure is related to the frequency Ω through

$$\Omega = \frac{(n-1)2\pi T}{N\,\Delta t}, \tag{7.1}$$

where Δt is the sampling interval and N the number of samples in the signal. There are three dominant frequencies: a low-frequency oscillation at $\Omega \approx 0.6$, the trapped-mode oscillation at $\Omega \approx 2.0$, and the higher-frequency oscillation at $\Omega \approx 2.8$ (there are other, much smaller, peaks at higher frequencies not included in this plot). The Fourier transform of the signal for $50T \leqslant t \leqslant 200T$ (not shown here) shows only two large peaks at $\Omega \approx 2.0$ and 2.8 with a virtually zero transform in the low-frequency range. It is the combination of oscillations at $\Omega \approx 2.0$ and 2.8 that is observable for larger times in figure 11(*a*). The low-frequency oscillation at $\Omega \approx 0.6$ is a pumping motion that dies out rapidly due to wave radiation. This motion is apparent for

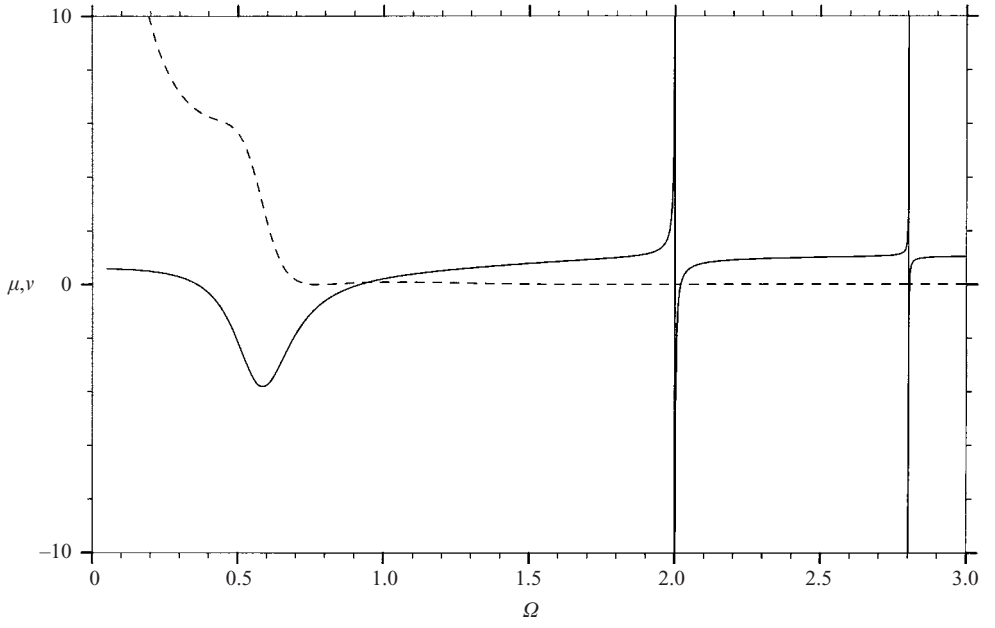

FIGURE 14. Non-dimensional added mass μ (———) and damping ν (– – – –) as a function of non-dimensional frequency $\Omega = \omega/\sqrt{g/h}$ for a sloshing-mode trapping structure.

smaller times in figure 11(*a*), and also in the snapshot of the free surface shown in figure 12(*a*), where the higher-frequency oscillations are 'riding' on the pumping motion.

As discussed in § 6, there is a strong link between the fluid motion as a function of time and variations in the added-mass coefficient that arises in the frequency-domain problem. A very rapid change in the added mass from large positive values to large negative values is associated with persistent oscillations in the time domain. Numerically computed values for this added mass, and for the corresponding damping coefficient, are shown as a function of frequency in figure 14 for the sloshing-mode trapping structure. There are very rapid changes in the added mass around $\Omega = 2.0$ and 2.8 corresponding to the persistent oscillations noted in the time domain. There is also a, less dramatic, region of negative added mass around $\Omega = 0.6$ which corresponds to the highly damped pumping motion. In addition, there are very localized anomalies in the damping coefficient around $\Omega = 2.0$ and 2.8, but these cannot be distinguished on the scale of figure 14.

It has been suggested (Evans & Porter 1998) that there is a correlation between the existence of a trapped mode for a two-element structure, and a zero of the transmission coefficient $\mathscr{T}$, at a nearby frequency, for an isolated element of that structure. Trapped modes arise when there is repeated perfect reflection of a wave between two such elements. Numerical computation of $\mathscr{T}$ for the structural element under discussion here shows that $\mathscr{T}$ has local minima very near zero for $\Omega \approx 1.97$ and 2.81 which are indeed close to the 'trapped-mode' frequencies found above.

8. Conclusion

The forced oscillations of a structure that supports a trapped mode have been examined in the time domain using asymptotic and numerical methods. Almost any

forcing, whether sustained or transitory, will excite the trapped mode and in the absence of friction it persists for all time.

Oscillatory forcing at the trapped-mode frequency produces fluid oscillations which grow with time but decay with space, as well as a certain amount of radiation of energy to infinity at the trapped-mode frequency. In contrast to this, a similar forcing at a frequency that differs from the trapped-mode frequency does not give rise to any growing oscillations, but rather generates a localized oscillation at the trapped-mode frequency as well as radiation at the forcing frequency. A transient forcing of the structure generates a bounded, localized oscillation at the trapped-mode frequency, which does not decay with time. This behaviour means that the usual assumption of linear water-wave theory, namely that after sufficient time there is only a steady-state oscillation at the forcing frequency, is incorrect for a trapping structure. For structures that support trapped modes, almost any initial condition or forcing will lead to persistent fluid oscillations at both the trapped-mode and forcing frequency. In particular, trapped modes will be excited by an incident mixed sea state.

An investigation was also made into the connection between the time- and frequency-domain solutions for both trapping and near-trapping structures. The trapping structure was given a sequence of perturbations which transformed it into two semicircular cylinders and the time-domain equations were solved for a transient, vertical forcing of the structure for each member of the sequence. For small perturbations of the trapping structure, localized oscillations are produced which have a frequency which is close to that of the trapped mode but with amplitude that decays slowly with time. Numerical estimates of the frequency and the rate of decay of the oscillation were made from the time-domain calculations. These values correspond to the real and imaginary parts of a pole in the complex force coefficient associated with the heave potential. An estimate of the position of this pole was obtained from calculations of the heave added mass and damping and good agreement with the time-domain results was found.

The calculations described in the previous paragraph are for a trapping structure with two elements that are quite close together. Further time-domain calculations for a trapping structure with more widely separated elements reveal fluid oscillations with two principal frequencies. These correspond to the constructed trapped mode and a second mode that is either another trapped mode, or a very lightly damped near-trapped mode. The numerical computations alone cannot distinguish between these two cases and a proof of the existence of a structure that supports trapped modes at more than one frequency has not yet been found.

This work was funded by grant number GR/M30937 awarded by the UK Engineering and Physical Sciences Research Council.

Appendix

Here the form of the heave potential in the vicinity of the trapped-mode frequency is derived for the structure illustrated in figure 2. This potential $\phi(x, z, \omega)$ satisfies Laplace's equation, the body boundary condition (3.6), the free-surface condition (3.7), a radiation condition, and has zero normal derivative on $z = -h$. Application of Green's theorem to ϕ and ϕ_0 for $\omega \neq \omega_0$ yields

$$\left(\omega^2 - \omega_0^2\right) \int_F \phi_0(\xi, 0)\phi(\xi, 0, \omega)\,\mathrm{d}x = -g \int_\Gamma \phi_0(\xi, \eta)\, n_\eta\,\mathrm{d}s. \tag{A 1}$$

The right-hand side of (A 1) may be determined numerically and it is non-zero. It is also independent of frequency, and so from the left-hand side of (A 1), there must be singularities in ϕ at $\omega = \pm\omega_0$. A Laurent series expansion for ϕ in the vicinity of $\omega = \omega_0$ is sought in the form

$$\phi(x, z, \omega) = \frac{\psi(x, z)}{\omega^2 - \omega_0^2} + \phi_1(x, z) + O(\omega - \omega_0) \quad \text{as} \quad \omega \to \omega_0. \tag{A 2}$$

This expansion is substituted into the governing equation and boundary conditions for ϕ and the coefficients of powers of $\omega - \omega_0$ are equated. Thus, ψ and ϕ_1 individually satisfy Laplace's equation. The body boundary condition (3.6) splits into the two conditions

$$\frac{\partial \psi}{\partial n} = 0 \qquad \text{and} \qquad \frac{\partial \phi_1}{\partial n} = n_\eta \qquad \text{on} \quad \Gamma \tag{A 3}$$

and the free-surface boundary condition (3.7) reduces to the two conditions

$$\frac{\omega_0^2}{g}\psi - \frac{\partial \psi}{\partial \eta} = 0 \qquad \text{and} \qquad \frac{\omega_0^2}{g}\phi_1 - \frac{\partial \phi_1}{\partial \eta} = -\frac{\psi}{g} \qquad \text{on} \quad \eta = 0. \tag{A 4}$$

Both ψ and ϕ_1 satisfy a radiation condition at frequency ω_0, which means that the Laurent expansion for ϕ must be non-uniform in x, as the exact radiation condition yields outgoing waves at frequency ω. However the function ψ satisfies the homogeneous boundary value problem at the trapped-mode frequency ω_0 and so it must be a multiple of the trapped-mode potential,

$$\psi = Ag\phi_0(x, z), \tag{A 5}$$

which decays as $|x| \to \pm\infty$. The strength A is determined from an expansion of (A 1), and is given by

$$A = \frac{-\displaystyle\int_\Gamma \phi_0(\xi, \eta)\, n_\eta \, \mathrm{d}\xi}{\displaystyle\int_F [\phi_0(\xi, 0)]^2 \, \mathrm{d}\xi}. \tag{A 6}$$

(Application of Green's theorem to ϕ_0 and the function $1 + \omega_0^2 z/g$ shows that the integral in the numerator may alternatively be written as

$$\int_\Gamma \phi_0(\xi, \eta)\, n_\eta \, \mathrm{d}\xi = \int_{-\infty}^{\infty} \phi_0(\xi, -h) \, \mathrm{d}\xi. \tag{A 7}$$

This alternative form is particularly useful in water of infinite depth, as the integral on the left-hand side of (A 7) is related to the coefficient of the vertical dipole in the expansion of ϕ_0 at large depths, and may be determined explicitly.) Substitution of (A 5) into (A 4) shows that ϕ_1 satisfies

$$\frac{\omega_0^2}{g}\phi_1 - \frac{\partial \phi_1}{\partial \eta} = -A\phi_0(\xi, 0) \qquad \text{on} \quad \eta = 0. \tag{A 8}$$

Thus ϕ_1 satisfies a forced boundary value problem at the trapped-mode frequency. From the Fredholm Alternative, the definition of A is sufficient to ensure existence of a solution for ϕ_1, and its uniqueness is guaranteed by the requirement of the constraint in (A 1) that

$$\int_F \phi_1(\xi, 0)\phi_0(\xi, 0) \, \mathrm{d}\xi = 0. \tag{A 9}$$

REFERENCES

Aslanyan, A., Parnovski, L. & Vassiliev, D. 2000 Complex resonances in acoustic waveguides. *Q. J. Mech. Appl. Maths* **53**, 429–447.

Bai, K. J. 1977 The added mass of two-dimensional cylinders heaving in water of finite depth. *J. Fluid Mech.* **81**, 85–105.

Clément, A. 1996 Coupling of two absorbing boundary conditions for 2D time-domain simulations of free surface gravity waves. *J. Comput. Phys.* **126**, 139–151.

Evans, D. V. & Porter, R. 1998 An example of non-uniqueness in the two-dimensional linear water-wave problem involving a submerged body. *Proc. R. Soc. Lond.* A **454**, 3145–3165.

Hazard, C. & Lenoir, M. 1993 Determination of scattering frequencies for an elastic floating body. *SIAM J. Math. Anal.* **24**, 1458–1514.

Isaacson, M. & Ng, J. Y. T. 1993 Time-domain second-order wave radiation in two dimensions. *J. Ship Res.* **37**, 25–33.

John, F. 1950 On the motion of floating bodies, II. *Commun. Pure Appl. Maths* **3**, 45–101.

Kennard, E. H. 1949 Generation of surface waves by a moving partition. *Q. Appl. Maths* **7**, 303–312.

Lenoir, M., Vullierme-Ledard, M. & Hazard, C. 1992 Variational formulations for the determination of resonant states in scattering problems. *SIAM J. Math. Anal.* **23**, 579–608.

Linton, C. M. & Evans, D. V. 1992 The radiation and scattering of surface waves by a vertical circular cylinder in a channel. *Phil. Trans. R. Soc. Lond.* A **338**, 325–357.

Linton, C. M. & Kuznetsov, N. G. 1997 Non-uniqueness in two-dimensional water wave problems: numerical evidence and geometrical restrictions. *Proc. R. Soc. Lond.* A **453**, 2437–2460.

Maiti, S. & Sen, D. 2001*a* Time-domain wave diffraction of two-dimensional single and twin hulls. *Ocean Engng* **28**, 639–665.

Maiti, S. & Sen, D. 2001*b* Nonlinear heave radiation forces on two-dimensional single and twin hulls. *Ocean Engng* **28**, 1031–1052.

Martin, P. A. & Farina, L. 1997 Radiation of water waves by a heaving submerged horizontal disc. *J. Fluid Mech.* **337**, 365–379.

Maskell, S. J. & Ursell, F. 1970 The transient motion of a floating body. *J. Fluid Mech.* **44**, 303–313.

McIver, M. 1996 An example of non-uniqueness in the two-dimensional linear water wave problem. *J. Fluid Mech.* **315**, 257–266.

McIver, M. 1997 Resonance in the unbounded water wave problem. In *Proc. 12th Intl Workshop on Water Waves and Floating Bodies, Carry-le-Rouet, France*, pp. 177–180.

McIver, M. 2003 The influence of a trapped mode on a radiation potential. *Proc. 18th Intl Workshop on Water Waves and Floating Bodies, Le Croisic, France* (ed. A. H. Clément & P. Ferrant).

McIver, M. & Porter, R. 2002 Trapping of waves by a submerged elliptical torus. *J. Fluid Mech.* **456**, 277–293.

McIver, P. 1994 Transient fluid motion due to the forced horizontal oscillations of a vertical cylinder. *Appl. Ocean Res.* **16**, 347–351.

McIver, P. & Linton C. M. 1991 The added mass of bodies heaving at low frequency in water of finite depth. *Appl. Ocean Res.* **13**, 12–17.

Newman, J. N. 1999 Radiation and diffraction analysis of the McIver toroid. *J. Engng Maths* **35**, 135–147.

Press, W. H., Teukolsky, S. A., Vetterling, W. T. & Flannery, B. P. 1992 *Numerical Recipes.* Cambridge University Press.

Sen, D. 1995 A cubic spline boundary integral method for two-dimensional free-surface flow problems. *Intl J. Numer. Meth. Engng* **38**, 1809–1830.

Simon, M. J. & Ursell, F. 1984 Uniqueness in linearized two-dimensional water-wave problems. *J. Fluid Mech.* **148**, 137–154.

Smith, C. M. 1982 The transient motion of a partially-immersed rolling strip in water. *IMA J. Appl. Maths* **29**, 59–77.

Ursell, F. 1964 The decay of the free motion of a floating body. *J. Fluid Mech.* **19**, 305–319.